

The proton-bound rare gas compounds (RgHRg)⁺ (Rg = Ar, Kr, Xe)—a computational approach

Jan Lundell,* Mika Pettersson and Markku Räsänen

Laboratory of Physical Chemistry, PO Box 55 (A.I. Virtasen aukio 1), FIN-00014 University of Helsinki, Finland. E-mail: lundell@csc.fi

Received 26th May 1999, Accepted 20th July 1999

Quantum chemical calculations have been performed on the various proton-bound rare gas dimers (RgHRg)⁺ where Rg = Ar, Kr or Xe. A good agreement is obtained with respect to the experimental data for the antisymmetric stretching wavenumbers of the three RgHRg⁺ cations. For the mixed (RgHRg)⁺ cations the computational results disagree with the recent experimental assignments (T. D. Fridgen and J. M. Parnis, *J. Chem. Phys.*, 1998, **109**, 2155) and a reassignment based on solvation of the centrosymmetric cations KrHKr⁺ and XeHXe⁺ is proposed.

Introduction

The protonated rare gas compounds RgHRg⁺ form an unusual family of molecular ions since they represent a prototype system for proton solvation by traditionally inert rare gas atoms. Although there have been a few experimental reports from the gas phase^{1,2} on ArHAr⁺ the major studies have been carried out in low-temperature rare gas matrices. The early observations of these cations date back to the early seventies when Ar_nH⁺ and Kr_nH⁺ were reported,^{3–5} and later the assignment to triatomic, centrosymmetric and linear ArHAr⁺, KrHKr⁺ and XeHXe⁺ cations was performed by Kunttu *et al.*^{6,7} They showed that after photodissociation of hydrogen halides in rare gas matrices the observed prominent $\nu_3 + n\nu_1$ progression is due to RgHRg⁺ species, which are isoelectronic with the bihalide ions XHX[−] (X = F, Cl, Br, I) exhibiting similar progression patterns.^{8,9}

The centrosymmetric cations RgHRg⁺ have prompted a wealth of computational studies.^{10–17} These studies employ methods ranging from DFT and MP2 *ab initio* calculations to analytical potential energy surface (PES) calculations and vibrational analysis probing the thermodynamic, structural and vibrational properties of these RgHRg⁺ cations. The vibrational analysis on XeHXe⁺¹² and ArHAr⁺¹³ indicate extensive mixing of the zeroth-order harmonic oscillator vibrational states. The major problem for computational studies, however, has been the large difference between the calculated harmonic vibrational wavenumbers and the experimental matrix data, the computational values exceeding the observed ν_3 wavenumbers by up to 30%. A classical MD study by Filippone and Gianturco¹⁸ reported an Ar(ArH⁺) complex instead of the centrosymmetric species, and since quantum effects were not included these simulations were unable to reproduce the structural properties acquired from *ab initio* calculations and the experimentally observed spectral characteristics of the centrosymmetric (Rg–H–Rg)⁺ cations.

Recently, an electron bombardment matrix isolation study¹⁹ of methanol–Rg mixtures appeared reporting experimentally for the first time the mixed cations ArHKr⁺, ArHXe⁺ and KrHXe⁺. These mixed rare-gas cations were first studied computationally by one of us using DFT theory.¹⁵ Additional computational reports using DFT theory^{16,17} have become available partly contradicting and

partly confirming the experimental assignments of Fridgen and Parnis.¹⁹ Therefore, we have reinvestigated the properties of the centrosymmetric and mixed protonated (RgHRg)⁺ (Rg = Ar, Kr, Xe) cations using highly correlated *ab initio* methods and large basis sets. Based on these new computational results we will suggest an alternative assignment of the matrix data indicating solvation of the symmetrical cationic species.

Computational methods

In this work, we have employed several approaches varying the basis sets and the level of theory. Most of the testing was done on the RgH⁺ (Rg = Ar, Kr, Xe) and ArHAr⁺ cations. We have chosen to report the results using the contracted 6-311G-type basis set augmented with several diffuse and polarization functions [6-311 + +G(3df,3pd)], but for example the 6-311 + +G(2d,2p) basis set gave comparable results. The all-electron basis sets were used for all atoms except xenon, which was treated by an 18 valence electron (VE) quasi-relativistic effective core potential (ECP) by LaJohn and co-workers.²⁰ This basis set was used in a decontracted form and is referred to as LJ18. This ECP has been previously demonstrated to be efficient and reasonably accurate for compounds containing xenon.^{21–23}

Electron correlation was treated by Møller–Plesset perturbation theory through second order (MP2), and also by single and double excitation coupled cluster methods including perturbative triples corrections [CCSD(T)]. For comparison, the hybrid Becke3 functional, which includes the Slater exchange along with corrections involving the gradient of the electron density (non-local exchange) was applied. The gradient-corrected LYP-functional was combined with the Becke3 exchange functional to give the B3LYP functional known to give reasonable results on a variety of chemical compounds. This computational approach was used to study the solvation of the centrosymmetric RgHRg⁺ cations due to the reduced computational cost compared to the other computational methods employed in this study.

All calculations were carried out within the framework of the GAUSSIAN 98²⁴ package of computer codes on the CRAY C94 and SGI Origin 2000 computers at the CSC-Center for Scientific Computing Ltd. (Espoo, Finland).

Results and discussion

Structural properties

To test the validity of the computational approach chosen, the results for the diatomic cations RgH^+ ($\text{Rg} = \text{Ar}, \text{Kr}$ or Xe) are compared with the experimental ones. For ArH^+ , the calculated bond distance is 1.2917, 1.2766 and 1.2789 Å at the B3LYP, MP2 and CCSD(T) levels, respectively, showing that improvement of the computational level gives results closer to the experimental value of 1.2804 Å²⁵ when correlation is increased. For KrH^+ the calculated bond distance is 1.4333, 1.4130 and 1.4212 Å at the B3LYP, MP2 and CCSD(T) levels, and the CCSD(T) value is exactly the same as presented for KrH^+ in the literature (1.4212 Å²⁵). The relativistic 18-VE ECP on Kr were found to give a rather short Kr–H bond distance of 1.3423 and 1.3442 Å for MP2 and CCSD(T), respectively. Due to the better accuracy of the non-relativistic all-electron basis set on Kr, which is still computationally affordable for the species studied here, the results for the 18-VE ECP on Kr have been omitted here.

For XeH^+ , where the 18-VE ECP is used for Xe, the calculated values of 1.6281, 1.5698 and 1.5742 Å at the B3LYP, MP2 and CCSD(T) levels, respectively, show a larger discrepancy compared to the experimental value of 1.6028 Å.²⁶ This is most likely due to basis set imbalance between the ECP on Xe and the highly polarized hydrogen basis set, and increasing especially the Xe ECP valence basis set and its flexibility should result in a closer agreement with the experimental values. This is in general agreement with results obtained for RgH^+ cations as well.²⁷

The computational structural properties of the rare-gas containing RgHRg^+ cations are collected in Table 1. A general trend is noted between the different computational approaches. For all diatomic cations the DFT calculations predict a longer bond distance than the CCSD(T) level, whereas the MP2 calculations show a tendency of a slightly shorter bond than the CCSD(T) calculation. Similarly, for the centrosymmetric RgHRg^+ cations the B3LYP calculations give longer Rg–H bond distances than the CCSD(T) calculations. The MP2 bond distances are close to the CCSD(T) values but slightly shorter. At the CCSD(T) level the Rg–H bond distances are 1.5018, 1.6624 and 1.8450 Å for Ar_2H^+ , Kr_2H^+ , and Xe_2H^+ , respectively.

The centrosymmetric RgHRg^+ cations possess a dissociation energy ($\text{RgHRg}^+ \rightarrow \text{RgH}^+ + \text{Rg}$) of ca. 62–66 kJ mol⁻¹ at the CCSD(T) level. This is similar to the result presented by Beyer *et al.*¹⁷ using the DFT theory. The formation of RgHRg^+ requires the attachment of a Rg atom to an already polarized RgH^+ cation, which results in a larger delocalization of the positive charge. The Mulliken population analysis at the MP2 level indicates a delocalized charge distribution on all the centrosymmetric cations in accord with previous computational studies on these species.^{12–17} Also, as noted in Table 1, there are only minor differences in dissociation energies obtained at various computational levels, and the B3LYP calculations give the largest dissociation energies for the centrosymmetric cations. These dissociation energies also explain why isolated RgH^+ cations have not been observed in solid matrices so far, and the exothermic reaction channel forming RgHRg^+ is always present.

A clear trend is found in all the mixed rare gas cations. The lighter rare gas atom shows a longer Rg–H bond distance than in the centrosymmetric species, whereas the heavier rare gas atoms possess a shorter Rg'–H bond distance than the corresponding centrosymmetric cation. This is in agreement with our previous results at the DFT and MP2 levels¹⁵ as well as the calculations of Beyer *et al.*¹⁷ However, the recent calculations by Fridgen and Parnis¹⁹ using the BP86/DN** level of theory predict the opposite and the authors anticipate that the use of extensive basis sets will give longer Rg–H bond distances for the heavier rare gases compared to shorter Rg–H bonds for the lighter rare gases. The results in Table 1 show clearly that this is not the case. Increasing the correlation and basis set flexibility favours the formation of a RgH^+ cation interacting with the smaller rare gas atom. This is understood on the basis of the lower ionization potential of the heavier rare gases. The most profound example is ArHXe^+ where the Ar–H distance is predicted to be ca. 2.02 Å, which is much longer than the CCSD(T) value of 1.5018 Å in ArHAr^+ . On the other hand, the Xe–H distance of 1.6071 Å is shorter than the calculated Xe–H bond distance of 1.8450 Å in XeHXe^+ , and it is only slightly larger than in XeH^+ . In addition, both MP2 and B3LYP results indicate that over 90% of the positive charge is localized on the XeH^+ subunit in ArHXe^+ . The weak interaction between the smaller rare gas atom and the RgH^+ subunit, involving a larger rare gas atom is highlighted in the calculated dissociation energies. Increasing the compu-

Table 1 Calculated structural and vibrational parameters for the linear $(\text{Rg}-\text{H}-\text{Rg}')^+$ cations. The LJ18 18-VE ECP was used on Xe and all other atoms were described by the 6-311 + G(3df,3pd) basis set

$(\text{RgHRg}')^+$		$r(\text{Rg}-\text{H})/\text{Å}$	$r(\text{H}-\text{Rg}')/\text{Å}$	ω_1/cm^{-1}	ω_2/cm^{-1} ^a	ω_3/cm^{-1}	$D_0/\text{kJ mol}^{-1}$ $(\text{RgHRg}')^+ \rightarrow$ $\text{RgH}^+ + \text{Rg}'$	$D_0/\text{kJ mol}^{-1}$ $(\text{RgHRg}')^+ \rightarrow$ $\text{Rg} + \text{Rg}'\text{H}^+$
ArHAr^+	B3LYP	1.5229		309.1	676.2(42)	1153.2(4326)	+74.88	
	MP2(full)	1.4965		331.5	729.8(43)	1102.4(4977)	+68.66	
	CCSD(T)	1.5018		328.8	723.5	1014.1	+64.32	
KrHKr^+	B3LYP	1.6851		198.3	620.0(18)	1153.1(4834)	+75.43	
	MP2(full)	1.6493		213.2	699.4(18)	1033.3(5856)	+71.18	
	CCSD(T)	1.6624		208.4	652.4	897.1	+62.58	
XeHXe^+	B3LYP	1.9075		140.5	550.5(1)	983.6(6067)	+72.86	
	MP2(full)	1.8409		157.4	617.5(1)	896.0(7806)	+67.73	
	CCSD(T)	1.8450		155.2	615.5	834.2	+66.05	
ArHKr^+	B3LYP	1.6424	1.5885	221.9(35)	625.3(28)	1209.8(4126)	+102.65	+52.29
	MP2(full)	1.6300	1.5468	221.0(67)	666.3(28)	1307.0(4696)	+98.83	+47.54
	CCSD(T)	1.6664	1.5424	198.5	633.4	1323.8	+91.99	+41.77
ArHXe^+	B2LYP	1.8700	1.7071	137.4(34)	472.5(11)	1568.7(2993)	+151.35	+27.87
	MP2(full)	1.9565	1.6123	111.2(26)	419.6(13)	1945.9(2188)	+172.07	+24.42
	CCSD(T)	2.0168	1.6071	101.3	377.8	2007.9	+179.19	+21.66
KrHXe^+	B3LYP	1.8809	1.7685	138.6(26)	531.5(6)	1311.4(4467)	+117.24	+44.11
	MP2(full)	1.9538	1.6535	112.6(37)	521.0(7)	1604.7(3979)	+134.17	+36.81
	CCSD(T)	2.0209	1.6403	98.6	477.2	1707.5	+138.34	+31.81

^a Doubly degenerate.

tational level decreases the $\text{Rg}-(\text{H}-\text{Rg}')^+$ dissociation energy, and the weakest interaction is found between Ar and XeH^+ where the smallest charge delocalization is observed. The CCSD(T)-calculated $\text{ArHXe}^+ \rightarrow \text{Ar} + \text{XeH}^+$ dissociation energy is *ca.* 22 kJ mol⁻¹.

Vibrational properties

The vibrational frequencies of the triatomic $(\text{RgHRg}')^+$ ($\text{Rg} = \text{Ar}, \text{Kr}, \text{Xe}$) cations are also collected in Table 1. The most distinct experimentally observable feature of these cations is the $\text{Rg}-\text{H}$ asymmetric stretch. For the centrosymmetric cations these absorptions have been measured at 904 (ArHAr^+), 854 (KrHKr^+) and 731 (XeHXe^+) in the corresponding pure rare gas solids.³⁻⁷ Additionally, all of these molecular ions show a prominent $\nu_3 + n\nu_1$ combination progression. The computational harmonic estimates of these vibrations have been generally several hundreds of wavenumbers higher than the experimental values from low-temperature matrices. Our best harmonic wavenumbers for the centrosymmetric cations are 1014, 897 and 834 cm⁻¹ for ArHAr^+ , KrHKr^+ and XeHXe^+ , respectively, at the CCSD(T) level. These values can be considered to be in a good agreement with the experimental values of 904, 854 and 731 cm⁻¹ in Ar, Kr and Xe, respectively. The difference in the experimental and calculated wavenumbers can be partly explained by the harmonic approximation neglecting anharmonic effects, but the solvation of the cations in a rare gas environment should also be taken into account. The good performance of the CCSD(T) calculations on the centrosymmetric RgHRg^+ cations suggests that this computational level can reliably be used to estimate the properties of the mixed $(\text{RgHRg}')^+$ species.

For the mixed rare gas cations the vibrational frequencies follow the RgH^+ subunit, and our calculated values for ω_3 are much higher than for the centrosymmetric cations. The CCSD(T) level predicts the cations ArHXe^+ , KrHXe^+ and ArHKr^+ to absorb at *ca.* 2008, 1708 and 1324 cm⁻¹, respectively. These values are several hundreds of wavenumbers higher than the BP86/DN** results used to interpret the experimental data on $(\text{RgHRg}')^+$ in low-temperature matrices.¹⁶ The computational properties of the mixed rare gas compounds seem to be quite similar at the various basis sets used in this study. The discrepancy between the BP86/DN** calculations¹⁶ and our CCSD(T) results must be attributed to the inadequate theoretical method used in the previous study. A comparison between the experimental and the CCSD(T) calculated vibrational frequencies is presented in Fig. 1. It is obvious that the vibrational bands originally assigned as mixed $(\text{RgHRg}')^+$ ^{16,19} are in a disagreement with our computational results, and another explanation should be looked for. In our opinion, a more plausible explanation is based on solvation of RgHRg^+ cations in different environments as will be discussed below.

Solvation of RgHRg^+ cations

According to the experimental data in low-temperature matrices¹⁹ there is rather continuous shift of the $\text{Rg}'\text{HRg}'^+ \nu_3$ band to higher wavenumbers upon doping the matrix with a lighter rare gas, Rg. When doping exceeds a few percent of Rg absorptions broaden and show structures indicating $\text{Rg}'\text{HRg}'^+$ in many different environments, *i.e.* one or more Rg' atoms are replaced by Rg in the solvation shell of $\text{Rg}'\text{HRg}'^+$. Finally, the band reaches the final position and it becomes narrower indicating the pure Rg environment. This behaviour is similar for all Rg, Rg' pairs.

Fridgen and Parnis¹⁹ assign the bands observed in Rg -matrices doped with a small amount of Rg' to mixed $(\text{RgHRg}')^+$ species. It should be noted that according to their

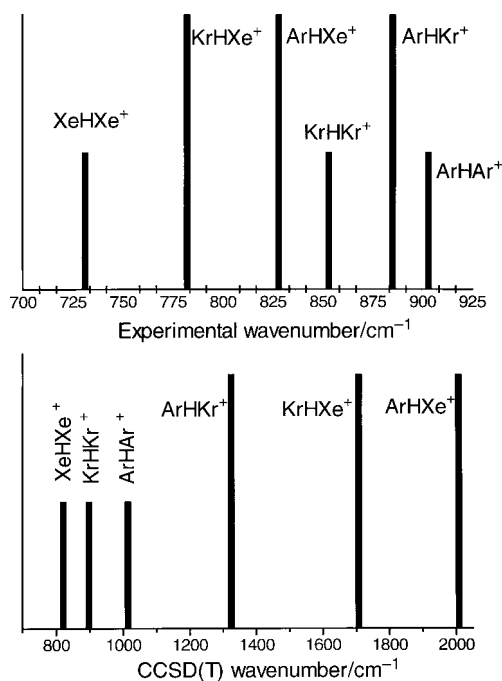


Fig. 1 A schematic comparison of the experimentally observed $(\text{RgHRg}')^+$ cations and their calculated harmonic ω_3 wavenumbers. Note the different wavenumber scales.

assignments the $(\text{RgHRg}')^+$ absorptions are *redshifted* from the corresponding centrosymmetric $(\text{RgHRg}')^+$ species by 16, 76 and 71 cm⁻¹ for ArHKr^+ , ArHXe^+ and KrHXe^+ , respectively. This assignment relies heavily on the BP86/DN** calculations on ArHKr^+ and the centrosymmetric species. In the case of ArHKr^+ the calculated shift is in a good agreement with the observed one but for the other mixed species the same computational level predicts strong *blueshifts*, which is in disagreement with the observations. Our CCSD(T) calculations show that even for ArHKr^+ the shift should be to the blue by about 300 cm⁻¹. Accordingly, we suggest that the bands at 885.3, 828.1 and 781.7 cm⁻¹ should be assigned to KrHKr^+ in Ar, XeHXe^+ in Ar, and XeHXe^+ in Kr, respectively. This assignment is supported not only by calculations but also by experimental evidence. The continuous shift of the $\text{Rg}'\text{HRg}'^+ \nu_3$ band upon various doping ratios indicates the same species in different environments. The final position is reached when $\text{Rg}'\text{HRg}'^+$ is isolated predominantly in a Rg environment. Secondly, for XeHXe^+ upon Ar and Kr doping also the $\nu_3 + n\nu_1$ progression shifts continuously, and even the intensity ratio of ν_1 and $\nu_3 + \nu_1$ seems rather similar to the pure Xe-matrix results. The $\nu_3 + n\nu_1$ progression being intensive up to $n = 5$ is characteristic of the centrosymmetric RgHRg^+ and their isoelectronic XHX^- ($\text{X} = \text{halogen}$) species, and it would be very surprising if the mixed $(\text{RgHRg}')^+$ possess a similar progression.

Our reassignments of the wavenumbers of the $\text{Rg}'\text{HRg}'^+$ cations in various low-temperature matrices are collected in Table 2. The values on the diagonal correspond to the experimental values in homogeneous matrices.^{6,7} All other values are from ref. 19. Clearly, the absorption bands shift according to the increasing polarizability of the environment.

In the mixed Ar–Kr matrix four bands were observed at 904, 885, 879 and 853 cm⁻¹. The bands at 904 and 853 cm⁻¹ belong to ArHAr^+ and KrHKr^+ in their respective homogeneous environments.⁷ The 885 cm⁻¹ band in an Ar matrix appears at a Kr/Ar ratio of 1/250 and reaches a maximum intensity at a ratio of 1/10. We propose that this band is due to KrHKr^+ in an Ar environment and its increase up to 10% doping can be explained by the enhanced probability of Kr-dimer formation in an Ar environment. Recently, Beyer *et*

Table 2 Assignment of the experimentally observed^a (RgHRg)⁺ ν_3 absorptions. The numbers in parentheses are the observed $\nu_3 + \nu_1$ absorptions (see text for details)

Environment	ArHAr ⁺	KrHKr ⁺	XeHXe ⁺
Ar	903.4(1140.1)	885.3	828.1(952.5)
Kr		853.2(1008.6)	781.7(900.3)
Xe			731.4(842.8)

^a The values on the diagonal are from refs. 6 and 7, and all other values are from ref. 19.

*al.*¹⁷ suggested that this 885 cm⁻¹ band could be due to Kr-shifted ArHAr⁺. In this case the shift induced by one additional Kr atom would be *ca.* 20 cm⁻¹, which is rather large to be induced by simple van der Waals interactions. For Ar–Xe and Kr–Xe mixtures this explanation seems even less probable because it would require ArHAr⁺ to shift by 76 cm⁻¹ upon complexation with Xe, and KrHKr⁺ to shift by 71 cm⁻¹ upon complexation with Xe. These values are clearly too large to corroborate this explanation. However, a tentative assignment of the 879 cm⁻¹ band as KrHKr⁺ with *one* additional Kr atom among the nearest neighbors can be made. Increasing the amount of Kr up to 90% enhances the band at *ca.* 858 cm⁻¹ that could tentatively be assigned as KrHKr⁺ with only one Ar atom in the near vicinity.

Similarly, the experimental data by Fridgen and Parnis assigned to ArHXe⁺ and KrHXe⁺ can be explained by solvation of the centrosymmetric cations. In the Ar–Xe experiments two bands at 828.1 and 952.5 cm⁻¹ appear at 1% Xe-doping, and can be attributed to ν_3 and $\nu_3 + \nu_1$ of XeHXe⁺ in a predominantly argon environment. These bands are separated by 124.4 cm⁻¹, which is slightly larger than found for XeHXe⁺ in pure Xe (111.4 cm⁻¹⁶). The two broad bands at 796 and 910 cm⁻¹ were originally assigned to XeHXe⁺ in pure Ar, but are more likely XeHXe⁺ in an heterogeneous environment, since these bands are quite profound at 20% Xe-doping ratio.

In the Kr–Xe matrices, the two bands at 781.7 and 900.3 cm⁻¹ appearing upon small Xe-doping can be assigned to XeHXe⁺ in a predominantly Kr environment. The broad bands at 765 and 875 cm⁻¹ belong to the same cation but in heterogeneous environment with one or several Xe atoms in the near vicinity. Note that the separation between ν_3 and $\nu_3 + \nu_1$ of XeHXe⁺ in Kr is 118.6 cm⁻¹, which is between the values of 111.4 and 124.4 cm⁻¹ in pure Xe and Ar, respectively. This indicates that the decreasing polarizability of the environment increases the ν_1 frequency of the rare gas cation. Also, according to these results, no lighter rare gas cations are found in heavier rare gas environments. This is also in accord with the computational dissociation energies presented in Table 1 and the preliminary report by one of us¹⁵ on RgHRg⁺ cations: the mixed rare gas species are not the major products in mixtures containing high mole fractions of heavier rare gases, since the reaction forming the centrosymmetric RgHRg⁺ cations are energetically favoured. However, the lighter rare gas matrices doped with a small amount of the heavier rare gases could still be a novel way to prepare the mixed (RgHRg)⁺ species in low-temperature matrices. Furthermore, experiments like those of Fridgen and Parnis using less than 1% doping of the heavier rare gas would be useful, and the calculated CCSD(T) frequencies presented in this study for the mixed (RgHRg)⁺ species should be very valuable for future efforts to isolate and characterize these species.

Finally, to test our new assignments of the experimental data we studied the solvation of KrHKr⁺ using the simplest possible model, *i.e.* the Onsager model employing a spherical cavity in a dielectric medium. The B3LYP/6-311++G(3df,3pd) level was used for all calculations due to its computational affordability compared to the other approaches in this

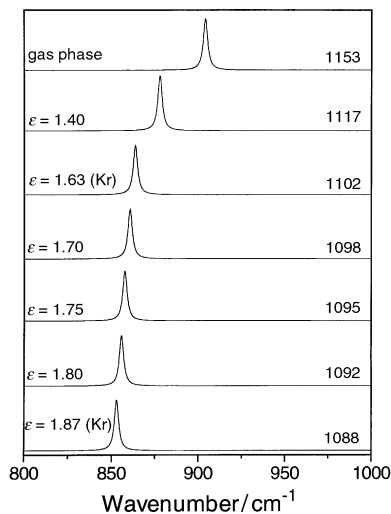


Fig. 2 The SCRF B3LYP/6-311++G(3df,3pd) calculated asymmetric stretch of Kr₂H⁺ using various relative permittivities. The frequencies are scaled using a scaling factor of 0.784. The numbers on the right-hand side are the unscaled frequencies (see text for details).

study. Fig. 2 shows the calculated asymmetric stretch of KrHKr⁺, when different relative permittivities going from the gas phase through Ar ($\epsilon = 1.63$) to Kr ($\epsilon = 1.87$),²⁸ are employed in the solvation model. Also, the calculated wavenumbers are scaled with a scaling factor of 0.784, which “normalizes” the ν_3 band of KrHKr⁺ in a Kr-environment to the experimental value of 853 cm⁻¹ measured in pure Kr matrix.⁷ It is interesting that decreasing the relative permittivity from 1.87 to 1.63 smoothly shifts the antisymmetric stretch upwards. This simple SCRF calculation predicts a shift of +14 cm⁻¹, which is in a qualitative agreement with the observed shift of +32 cm⁻¹.

Conclusions

Quantum chemical calculations on the structures, energetics and vibrational properties of RgHRg⁺ and (RgHRg)⁺ where Rg = Rg' = Ar, Kr or Xe have been performed using B3LYP, MP2 and CCSD(T) levels of theory employing large and flexible basis sets. For the centrosymmetric RgHRg⁺ cations the predicted wavenumbers for the antisymmetric stretch (ν_3) are in correct qualitative agreement with experimental values obtained from matrix isolation experiments. However, the calculated wavenumbers for the mixed triatomic cations show that these cations should absorb several hundreds of wavenumbers higher than the centrosymmetric cations. This contradicts the previous experimental assignment of these mixed (RgHRg)⁺ cations and supports the conclusions made by Beyer *et al.*¹⁷ Based on our calculations the new experimental bands originate from solvated centrosymmetric RgHRg⁺ cations in different environments. SCRF calculations employing a simple Onsager model with a cavity in a dielectric medium are able to qualitatively reproduce the experimental shifts of KrHKr⁺ in various solvents in agreement with experimental data. The calculated wavenumbers for the mixed rare gas cations are valuable for further studies of doubly-doped rare gas matrices aiding the experimental observation of the ArHKr⁺, ArHXe⁺ and KrHXe⁺ cations, and these experiments are strongly encouraged.

Acknowledgements

The Academy of Finland is thanked for financial support and the CSC-Center for Scientific Computing Ltd. is thanked for computer mainframe time spent during this study. Prof. V. E.

Bondybey is thanked for making ref. 17 available prior to publication and for valuable comments on the manuscript.

References

- 1 N. G. Adams, D. K. Bohme and E. E. Ferguson, *J. Chem. Phys.*, 1970, **52**, 5101.
- 2 G. Hvistendahl, O. W. Saastad and G. Uggerud, *Int. J. Mass Spectrom. Ion Processes*, 1980, **98**, 167 and references therein.
- 3 V. E. Bondybey and G. Pimentel, *J. Chem. Phys.*, 1972, **56**, 3832.
- 4 D. E. Milligan and M. E. Jacox, *J. Mol. Spectrosc.*, 1973, **46**, 460.
- 5 C. A. Wight, B. S. Ault and L. Andrews, *J. Chem. Phys.*, 1976, **65**, 1244.
- 6 H. Kunttu, J. Seetula, M. Räsänen and V. A. Apkarian, *J. Chem. Phys.*, 1992, **96**, 5630.
- 7 H. M. Kunttu and J. A. Seetula, *Chem. Phys.*, 1994, **189**, 273.
- 8 B. S. Ault, *Acc. Chem. Res.*, 1982, **15**, 103 and references therein.
- 9 M. Räsänen, J. Seetula and H. Kunttu, *J. Chem. Phys.*, 1993, **98**, 3914.
- 10 S. G. Potapov, L. P. Sukhanov and G. L. Gutsev, *Russ. J. Phys. Chem.*, 1989, **63**, 479.
- 11 M. E. Rosenkrantz, *Chem. Phys. Lett.*, 1990, **173**, 378.
- 12 J. Lundell and H. Kunttu, *J. Phys. Chem.*, 1992, **96**, 9774.
- 13 J. Nieminen, E. Kauppi, J. Lundell and H. Kunttu, *J. Chem. Phys.*, 1993, **98**, 8698.
- 14 J. Nieminen and E. Kauppi, *Chem. Phys. Lett.*, 1994, **217**, 31.
- 15 J. Lundell, *J. Mol. Struct.*, 1995, **355**, 291.
- 16 T. D. Fridgen and J. M. Parnis, *J. Chem. Phys.*, 1998, **109**, 2162.
- 17 M. Beyer, A. Lammers, E. V. Savchenko, G. Niedner-Schatteburg and V. E. Bondybey, *Phys. Chem. Chem. Phys.*, 1999, **1**, 2213.
- 18 F. Filipponi and F. A. Gianturco, *Europhys. Lett.*, 1998, **44**, 585.
- 19 T. D. Fridgen and J. M. Parnis, *J. Chem. Phys.*, 1998, **109**, 2155.
- 20 L. A. LaJohn, P. A. Christiansen, R. B. Ross, T. Atashroo and W. C. Ermler, *J. Chem. Phys.*, 1987, **87**, 2812.
- 21 M. Pettersson, J. Lundell, L. Khriachtchev, E. Isoniemi and M. Räsänen, *J. Am. Chem. Soc.*, 1998, **120**, 7979.
- 22 M. Pettersson, J. Lundell, L. Khriachtchev and M. Räsänen, *J. Chem. Phys.*, 1998, **109**, 618.
- 23 M. Pettersson, J. Lundell and M. Räsänen, *Eur. J. Inorg. Chem.*, 1999, 729.
- 24 M. J. Frisch, G. W. Trucks, H. B. Schlegel, G. E. Scuseria, M. A. Robb, J. R. Cheeseman, V. G. Zakrzewski, J. A. Montgomery, Jr., R. E. Stratmann, J. C. Burant, S. Dapprich, J. M. Millam, A. D. Daniels, K. N. Kudin, M. C. Strain, O. Farkas, J. Tomasi, V. Barone, M. Cossi, R. Cammi, B. Mennucci, C. Pomelli, C. Adamo, S. Clifford, J. Ochterski, G. A. Petersson, P. Y. Ayala, Q. Cui, K. Morokuma, D. K. Malick, A. D. Rabuck, K. Raghavachari, J. B. Foresman, J. Cioslowski, J. V. Ortiz, B. B. Stefanov, G. Liu, A. Liashenko, P. Piskorz, I. Komaromi, R. Gomperts, R. L. Martin, D. J. Fox, T. Keith, M. A. Al-Laham, C. Y. Peng, A. Nanayakkara, C. Gonzalez, M. Challacombe, P. M. W. Gill, B. Johnson, W. Chen, M. W. Wong, J. L. Andres, C. Gonzalez, M. Head-Gordon, E. S. Replogle and J. A. Pople, GAUSSIAN 98, Revision A.3, Gaussian Inc., Pittsburgh, PA, 1998.
- 25 J. W. C. Johns, *J. Mol. Spectrosc.*, 1984, **106**, 124.
- 26 S. A. Rogers, C. R. Brazier and P. F. Bernath, *J. Chem. Phys.*, 1987, **87**, 159.
- 27 J. Lundell, J. Nieminen and H. Kunttu, *Chem. Phys. Lett.*, 1993, **208**, 247.
- 28 R. L. Amey and R. H. Cole, *J. Chem. Phys.*, 1964, **40**, 146.

Paper 9/04242C